

# **Paclitaxel Sensitivity of Ovarian Cancer can be enhanced by knocking down Pairs of Kinases that regulate MAP4 Phosphorylation and Microtubule Stability**

Hailing Yang<sup>1</sup>, Weiqun Mao<sup>1</sup>, Cristian Rodriguez-Aguayo<sup>1,3</sup>, Lingegowda S. Mangala<sup>2,3</sup>, Geoffrey Bartholomeusz<sup>1</sup>, Lakesia R. Iles<sup>1</sup>, Nicholas B. Jennings<sup>3</sup>, Ahmed Ashour Ahmed<sup>4,5</sup>, Anil K. Sood<sup>2,3</sup>, Gabriel Lopez-Berestein<sup>1,3</sup>, Zhen Lu<sup>1\*</sup>, and Robert C. Bast, Jr.<sup>1\*</sup>

Departments of <sup>1</sup>Experimental Therapeutics and <sup>2</sup>Gynecologic Oncology and Reproductive Medicine, and <sup>3</sup>Center for RNA Interference and Non-Coding RNA, University of Texas, M.D. Anderson Cancer Center, Houston, TX 77030. <sup>4</sup>Ovarian Cancer Cell Laboratory, Weatherall Institute of Molecular Medicine, University of Oxford, Headington, Oxford, OX3 9DS, UK and <sup>5</sup>Nuffield Department of Women's & Reproductive Health, University of Oxford, Women's Centre, John Radcliffe Hospital, Oxford, OX3 9DU, UK.

\*Co-senior authors:

**Correspondence to:** Robert C. Bast Jr, MD, and Zhen Lu, MD, Department of Experimental Therapeutics, University of Texas MD Anderson Cancer Center, Unit 1439, 1400 Pressler Street, Houston, TX, 77030, USA; phone: 713-792-7743; FAX: 713-792-7864, e-mail: [rbast@mdanderson.org](mailto:rbast@mdanderson.org) and [zlu@mdanderson.org](mailto:zlu@mdanderson.org)

**Running title:** Combinatorial siRNA therapy enhances Paclitaxel sensitivity

**Key words:** Ovarian Cancer; siRNA, microtubule, paclitaxel and kinase

## **Abstract**

**Purpose:** Most ovarian cancer patients receive paclitaxel chemotherapy, but less than half respond. Pre-treatment microtubule stability correlates with paclitaxel response in ovarian cancer cell lines. Microtubule stability can be increased by depletion of individual kinases. As microtubule stability can be regulated by phosphorylation of microtubule associated proteins (MAPs), we reasoned that depletion of pairs of kinases that regulate phosphorylation of MAPs could induce microtubule stabilization and paclitaxel sensitization.

**Experimental Design:** Fourteen kinases known to regulate paclitaxel sensitivity were depleted individually in 12 well-characterized ovarian cancer cell lines before measuring proliferation in the presence or absence of paclitaxel. Similar studies were performed by depleting all possible pairs of kinases in 6 ovarian cancer cell lines. Pairs that enhanced paclitaxel sensitivity across multiple cell lines were studied in depth in cell culture and in two xenograft models.

**Results:** Transfection of siRNA against 10 of the 14 kinases enhanced paclitaxel sensitivity in at least 6 of 12 cell lines. Dual knockdown of IKBKB/STK39 or EDN2/TBK1 enhanced paclitaxel sensitivity more than silencing single kinases. Sequential knockdown was superior to concurrent knockdown. Dual silencing of IKBKB/STK39 or EDN2/TBK1 stabilized microtubules by inhibiting phosphorylation of p38 and MAP4, inducing apoptosis and blocking cell cycle more effectively than silencing individual kinases. Knockdown of IKBKB/STK39 or EDN2/TBK1 enhanced paclitaxel sensitivity in two ovarian xenograft models.

**Conclusions:** Sequential knockdown of dual kinases increased microtubule stability by decreasing p38-mediated phosphorylation of MAP4 and enhanced response to paclitaxel in ovarian cancer cell lines and xenografts, suggesting a strategy to improve primary therapy.

## **Translational relevance**

Most patients with newly diagnosed ovarian cancer are treated with a combination of paclitaxel and carboplatin. While 70% of ovarian cancers respond to carboplatin, less than 50% respond to paclitaxel as a single agent and synergy is not observed between the two drugs. Thus, primary resistance to paclitaxel is a major obstacle to successful treatment. Our previous studies documented that resistance is relative and can be reduced by enhancing microtubule stability by silencing certain kinases. This study documents the impact of sequentially silencing IKBKB and STK39 or EDN2 and TBK1 on paclitaxel sensitivity, providing a rationale for siRNA-based therapy. Different siRNAs are in the developmental pipeline and more than a dozen are in phase I or II clinical trials. Our results also support the development of small molecule inhibitors of the NFkB pathway, EDN2 and TBK1. Either approach could enhance primary paclitaxel-based therapy for ovarian cancer and improve patient outcomes.

## Introduction

Ovarian cancer continues to be the leading cause of gynecologic cancer deaths in the United States (1). Over the last three decades, the 5-year survival has improved significantly to approximately 50% with optimal care, but the rate of cure has not changed, remaining at less than 30% when all stages are included. Following cytoreductive surgery, most newly diagnosed ovarian cancer patients are treated with a combination of carboplatin and paclitaxel. While 70% of newly diagnosed ovarian cancers will respond to a platinum compound with or without paclitaxel, only 42% of cancers responded to paclitaxel alone in the Gynecologic Oncology Group (GOG) trial 132 (2,3). The addition of paclitaxel to platinum compounds did, however, improve survival in two of three pivotal studies (4). As synergy is not observed between platinum compounds and taxanes, less than half of patients benefit from the addition of paclitaxel to carboplatin. Better outcomes might be attained if the primary response to paclitaxel could be enhanced.

Paclitaxel binds to  $\beta$ -tubulin, stabilizes microtubules by inhibiting microtubule depolymerization, impairs mitotic spindle formation, arrests mitosis and induces apoptosis (5). Because paclitaxel only binds to preformed microtubules, the pre-treatment state of microtubules is an important determinant of the magnitude of paclitaxel-induced microtubule stabilization and cytotoxicity. For example, mutations outside the binding sites of paclitaxel that increases microtubule dynamic instability induces resistance to paclitaxel (6). In contrast, culturing ovarian cancer cells on TGFBI-coated plates enhanced microtubule stability and paclitaxel-induced cytotoxicity (7). Our previous studies documented that enhancing baseline microtubule stability increased paclitaxel-induced microtubule stabilization and the ability of paclitaxel to induce apoptosis (6,8). Depletion or inhibition of certain kinases could increase microtubule stability and enhance the apoptotic response to paclitaxel (8,9). As microtubule stability is regulated by microtubule associated proteins (MAPs) and phosphorylation of MAPs affects their binding to microtubules, it is likely that at least some of these effects might be regulated by kinases that regulate MAP phosphorylation (10).

From a previous siRNA kinome screen, 14 candidate kinases were selected for further study whose silencing enhanced paclitaxel sensitivity and in some cases enhanced microtubule stability in SKOv3 ovarian cancer cells (11). These 14 target kinases were validated by measuring the IC<sub>50</sub> in ovarian cancer cell lines with different molecular abnormalities. To identify combinations of kinases whose silencing would have an even greater effect on paclitaxel sensitivity, all possible pairs were tested against 6 ovarian cancer cell lines in the presence and absence of paclitaxel. Two pairs of siRNAs (IKBKB/STK39 and END2/TBK1) consistently increased paclitaxel sensitivity in multiple ovarian cancer cell lines. Sequential depletion of IKBKB and STK39 or END2 and TBK1 kinases significantly increased paclitaxel sensitivity in cell culture, enhanced microtubule stability and produced cell cycle arrest and apoptosis in the presence of paclitaxel. Silencing of IKBKB and STK39 or EDN2 and TBK1 enhanced paclitaxel sensitivity in xenograft models, suggesting that silencing of these kinases with siRNA or small molecule inhibitors could provide a strategy to improve ovarian cancer patient outcomes in the clinic.

## MATERIAL AND METHODS

**Cells and culture conditions.** The sources of ovarian cancer cell lines (A2780, CaOv3, EFO21, EFO27, HeyA8, IGORV1, OAW42, OC316, OVCAR3, OVCAR5, SKOv3ip, SW626 and UPN251)

and culture media are listed in **Table S1**. Culture media were supplemented with 10% FBS and 200  $\mu$ M L-glutamine. Cells were incubated at 37°C with 5% CO<sub>2</sub>, except for SW626 which was grown without CO<sub>2</sub> supplementation. Cell lines were genetically fingerprinted by the MD Anderson CCSG Core Facility to assure their authenticity. Genetic mutations of cell lines (p53, BRCA1 or BRCA2) were listed in **Table S1**.

**siRNA transfection in cultured cells.** Dharmacon siGENOME siRNA was transfected according to the manufacturer's instructions. For single transfections, 3000-8000 cells were reversely transfected in each well of a 96-well plate. For two sequential transfections, 4500 SKOv3ip cells, 3500 HeyA8 cells or 5000 OVCAR5 cells were reversely transfected on day 1 and then forwardly transfected on day 2. Final siRNA concentration was 25 nM per well in antibiotic-free media. The siRNA catalogue numbers are shown in **Table S2**.

**Real-time PCR.** RNA was extracted using the Trizol method (Life Technology). 1  $\mu$ g cDNA was synthesized using iScript™ Select cDNA Synthesis Kit by Bio-Rad. qRT-PCR was performed using CFX Connect Real-time System (Bio-Rad, Hercules, CA). Data were calculated using the  $\Delta\Delta$ Ct method. GAPDH was used as a reference gene. Experiments were carried out in triplicate and repeated twice. Primer sequences are shown in **Table S3**.

**Custom siRNA screen.** To determine optimal transfection conditions, a variety of transfection reagents, non-targeting control siRNAs and positive control siRNAs were tested on A2780, CaOv3, EFO27, HeyA8, OAW42 and SKOv3 cell lines. Paclitaxel was titrated in each cell line to determine an IC<sub>25</sub>. The optimal reagents and paclitaxel concentration for screens for each cell line are listed in **Table S4**. Cells were reverse transfected with an initial siRNA in a 96-well black-walled plates in triplicates. After 24 hrs, a second siRNA was transfected. Cells were treated with paclitaxel 48 hrs after the final transfection and incubated for another 72 hrs. Cell viability was analysed using a sulforhodamine B assay as described below. All plates were normalized to values for untreated cells to eliminate plate differences. Sample values were averaged and the ratios of paclitaxel treated (+) to untreated (-) cultures were calculated. The ratio of paclitaxel treated to non-treated cells incubated with the targeted siRNA was compared to the ratio of paclitaxel treated to non-treated cells incubated with the non-targeted siRNA control. A difference of > 0.5 fold was selected for further evaluation. A heatmap was generated using median-centered fold changes for paclitaxel sensitivity. The fold-changes of each kinase siRNA were calculated using the ratio of the SRB assay value normalized to control siRNA with and without paclitaxel treatment. The heat map generated from normalized fold-changes displays the differences of the z-scores, which were calculated using Cluster 3 (Stanford University) and Treeview (Alok Saldanha's) open source software.

**Sulforhodamine B assay.** Cells were transfected and treated with paclitaxel or diluent in 96-well plates as described in *in vitro* siRNA delivery, fixed with 30% (v/v) trichloroacetic acid for 30 min at 4°C, and stained with 0.1% (w/v) sulforhodamine B in 1% (v/v) acetic acid. The dye was extracted using 100  $\mu$ L of 10 mM Tris at pH 8.0 and the optical density read at 570 nm. Data were log transformed, normalized to the diluent control, and then fitted to a least squares curve using GraphPad Prism 6 software (GraphPad Software, Inc). Experiments were performed in quadruplicate and repeated at least twice.



**Western blot.** To measure knockdown efficiency and protein phosphorylation, cells were lysed for 30 min at 4°C. For microtubule stability experiments, to measure microtubule detubulin, cells were washed with PBS at 37°C and lysed in boiling SDS lysis buffer. For microtubule fractionation assays, cells were lysed in a microtubule stabilizing buffer (20 mM Tris-HCl pH 6.8, 0.14 M NaCl, 2 mM EGTA, 1 mM MgCl<sub>2</sub>, 0.5% Triton X-100 and 4 μM paclitaxel) for 30 min on ice. Lysates were centrifuged at 12,000 g for 10 min at 4 °C to separate microtubule polymers in pellet (P) and free soluble tubulin dimers in supernatant (S). Both fractions were run side by side on SDS-PAGE gels. Tubulin and GAPDH were blotted using specific antibodies. The density of tubulin bands in S and P fractions were determined by Image J and the microtubule fraction (%) is calculated by  $P/(S+P) \times 100\%$ . GAPDH is soluble in the supernatant fraction. Here we used it to assure no contamination of supernatant and pellet fractions. All samples were separated by 8% SDS-PAGE. The source of antibodies is detailed in **Table S5**.

**Apoptosis and cell cycle analyses.** Cells transfected with targeted or control siRNA and treated with paclitaxel or diluent were detached with 0.25% trypsin. For apoptosis analysis,  $1 \times 10^5$  cells were stained for 30 min at room temperature using Alexa 488 conjugated annexin V and propidium iodide (PI) from a Dead Cell Apoptosis Kit from Fisher. For cell cycle analysis,  $1 \times 10^5$  cells were stained with 10 μg/ml PI after fixation in 70% ice cold ethanol. Cells were analyzed with a Gallios Cell Analyzer from Beckman Coulter, Inc. (Brea, CA).

**siRNA liposomal preparation.** siRNA for *in vivo* studies was incorporated into neutral liposomes, with 1,2-dioleoyl-*sn*-glycero-3-phosphatidylcholine (DOPC) as described in (11). siRNAs (Sigma, custom siRNA duplex) and DOPC were mixed at a ratio of 1:10 (w/w) in excess tertiary butanol. Tween 20 was added to the mixture in a ratio of 1:19 (v/v). The mixture was vortexed, frozen in acetone on a dry ice bath, and then lyophilized. siRNA-DOPC was reconstituted in 200 uL room temperature PBS without calcium or magnesium immediately before injection.

**Xenograft studies.** Experiments with athymic nu/nu-Foxn1 mice (Envigo) were reviewed and approved by the Institutional Animal Care and Use Committee of M. D. Anderson Cancer Center (IACUC ID: 00001052). Female mice of 6 weeks of age were injected i.p. with  $1 \times 10^6$  SKOV3ip or  $1 \times 10^6$  OVCAR5 ovarian cancer cells. Mice were randomized into groups of 10. Treatment was initiated 1-week after cancer cell injection, for the following groups: 1) non-targeting control siRNA, 2) control siRNA and paclitaxel, 3) siRNA #1, 4) siRNA #1 and paclitaxel, 5) siRNA #2, 6) siRNA #2 and paclitaxel, 7) combination of both siRNAs, 8) combination of both siRNAs and paclitaxel. siRNA was administered i.p. biweekly at 10 ug per mouse. Paclitaxel was administered once a week at a dose of 1 mg/kg per mouse for SKOV3ip and 3 mg/kg for OVCAR5 immediately following siRNA treatment. Mice were treated for approximately 5 weeks until mice in any single group became moribund. All mice were sacrificed and assessed for tumor burden by excising and weighing i.p. tumor nodules.

**Human tumor tissue arrays and their analysis.** Tissue sections of normal ovary duplicate sections of ovarian cancer tissue arrays were acquired from the MD Anderson Pathology Core. Slides were incubated at 56°C for 1 hr, passed through xylene to remove paraffin, and rehydrated through decreasing concentrations of ethanol. Antigens were retrieved using Diva decloaker in a pressure cooker at 110°C for 10 min and 90°C for 2 min. Samples were blocked with PeroxAbolish, according to manufacturer's instruction. Samples were then blocked with 5% BSA

in PBS for 30 min followed by incubation with primary antibody against either IKBKB at 1:20 dilution (Cell Signaling Technology) or STK39 at 1:500 dilution (Abcam) overnight at 4°C. After PBS wash, slides were incubated with 4PLUS biotinylated goat anti rabbit IgG and 4PLUS streptavidin HRP label. Slides were developed using Betazoid DAB chromogen kit and counterstained with CAT hematoxylin. All reagents were purchased from BioCare Medical. Slides were scored by two researchers independently (ZL and HY). Cores with no specific protein expression were recorded as 0, low expression as 1, moderate expression as 2 and high expression as 3. A total of 219 cases qualified for this analysis. The histotypes and stages of tumor cases was listed in Table S8.

**Statistical analysis.** Data are represented as means +/- standard deviations unless otherwise specified. Statistical significance was determined by an independent sample Mann-Whitney U test or t-test. The minimal level of significance was  $p < 0.05$ .

## RESULTS

**siRNA mediated knockdown of 14 distinct kinases potentiates paclitaxel sensitivity across multiple ovarian cancer cell lines with WT and mutant TP53, BRCA1 and BRCA2.** From a previous siRNA kinome screen in SKOV3 ovarian cancer cells, 14 candidate kinases were identified whose knockdown enhanced paclitaxel sensitivity, including AATK, ACRBP, BMP2K, CHUK, EDN2, IKBKB, ILK2, RAPGEF3, RAPGEF4, SIK2, STK24, STK39, TBK1 and TRIM27. To validate the ability of these kinases to regulate paclitaxel sensitivity across multiple ovarian cancer cell lines, the IC<sub>50</sub> of paclitaxel was measured after treatment with specific kinase siRNAs and with control siRNAs in each of 12 well characterized cell lines, including A2780, CaOV3, EFO21, EFO27, HeyA8, IGROV1, OAW42, OC316, OVCAR3, SKOV3ip, SW626 and UPN251. Different ovarian cancer cell lines expressed both wild type and mutant TP53, BRCA1 and BRCA2. These mutations are often viewed as the biomarkers for high-grade serous ovarian cancer (**Table S1**). When the ratio of control siRNA to kinase siRNA was calculated, knockdown of each of the 14 kinases significantly enhanced paclitaxel sensitivity from 2 cell lines (AATK) to all 12 cell lines (STK39) (**Table S6**). siRNAs against seven kinases (ACRBP, CHUK, EDN2, IKBKB, RAPGEF3, TRIM27 and SIK2) increased paclitaxel sensitivity in more than half of ovarian cancer cell lines tested. The most marked potentiation (6.25 fold) was observed in OC316 cells with SIK2. TBK1 siRNA increased paclitaxel sensitivity >1.5 fold in 5 cell lines, siACRBP in 6 cell lines, siCHUK in 8 cell lines, siIKBKB in 8 cell lines, siRAPGEF3 in 6 cell lines, siSIK2 in 8 cell lines, siSTK39 in 8 cell line and siTRIM in 6 cell lines (**Table S6**). Previous reports suggest that 9 of the 14 Kinases (ACRBP, CHUK, EDN2, IKBKB, ILK2, TRIM27, SIK2, STK39 and TBK1) are overexpressed in different ovarian cancers (12-22), and similarly, TCGA analysis shows upregulation at the mRNA level for all 14 kinases ranging from 1.6%-25% (cBioPortal). Modulating the activity of kinases that are overexpressed in ovarian cancers may provide a therapeutic window to improve the activity of paclitaxel in patients with ovarian cancer. Thus, several kinases show promise across diverse ovarian cancer cell lines. While the number of cell lines with particular mutations was small, there was no apparent correlation between the particular mutations and the effect of kinase knockdown on paclitaxel sensitivity.

**Depletion of EDN2, IKBKB, SIK2 or STK39 expression enhances microtubule stability.** Enhanced sensitivity to paclitaxel could arise through several different mechanisms including enhanced microtubule stability. To understand the underlying mechanisms by which 14 siRNAs

enhancing paclitaxel sensitivity, we tested microtubule stability/dynamics in the SKOV3ip ovarian cancer cell line by knocking down each of the 14 kinases individually using pooled siRNAs (8). Detyrosinated  $\alpha$ -tubulin (also called glu-tubulin) is a marker for stable microtubules that also increases following paclitaxel treatment in a dose-dependent manner (23). To determine microtubule stability, we measured the levels of detyrosinated tubulin by Western Blot in SKOV3 cells and found that siRNAs against EDN2, IKBKB, SIK2 and STK39 dramatically increased the levels of glu-tubulin, indicating that these siRNAs stabilized microtubules (**Figure 1A and 1C**). Downregulation of the other ten kinases (AATK, ACRBP, BMP2K, CHUK, ILK, RAPGEF3, RAPGEF4, STIK24, TBK1 and TRIM27) using siRNA failed to affect microtubule stability (**Figure 1B and 1C**), although similar knockdown efficiency was achieved compared to siEDN2, siIKBKB, siIK2 and siSTK39 (**Figure 1D**). Similar results were observed when HeyA8 cells were treated with individual siRNAs (**Figure S1A-C**). Thus, silencing of EDN2, IKBKB, SIK2 or STK39 enhanced paclitaxel sensitivity and increased microtubule stability, whereas the other 10 siRNAs apparently rely on other mechanisms to enhance paclitaxel sensitivity in ovarian cancers.

**Depletion of pairs of kinases further enhances paclitaxel sensitivity.** To test whether further stabilization of microtubules and enhancement of paclitaxel sensitivity could be attained by knockdown of multiple kinases, we extended our siRNA screen to study treatment with combinations of two siRNAs in six ovarian cancer cell lines (A2780, CaOv3, EFO21, HeyA8 OAW42 and SKOV3ip). We used a protocol that changed both the order and interval of dual siRNA addition, in which the first siRNA was reversely transfected for 24 hrs followed by the second siRNA transfection for 24 hrs, followed, in turn, by the addition of a single dose of paclitaxel for an additional 72 hrs. Use of siRNAs against two different kinases in combination enhanced paclitaxel sensitivity in some cases, but decreased paclitaxel sensitivity in others. A heat-map was generated to represent median-centered fold change of paclitaxel sensitivity in different ovarian cancer cell lines (**Figure 2A and Table S7**). By inspection of the heat-map it is apparent that silencing of IKBKB and STK39 or of EDN2 and TBK1 provided the most consistent enhancement of paclitaxel sensitivity across the 6 cell lines. IKBKB siRNA followed by STK39 siRNA (IKBKB-STK39) significantly enhanced paclitaxel activity in all six cell lines with a >1.5 fold increase in paclitaxel sensitivity in 4 of the 6 (**Table S7**). Similarly, EDN2 siRNA followed by TBK1 siRNA (EDN2-TBK1) enhanced paclitaxel sensitivity in 3 of the 6 cell lines with a >1.5 fold increase in paclitaxel sensitivity in 3 of the 6. Based on these data and the fact that 3 of the 4 kinases regulated microtubule stability (IKBKB, STK39, EDN2 and TBK1), we chose IKBKB/STK39 siRNAs and EDN2/TBK1 siRNAs for further evaluation.

**Sequential depletion of IKBKB and STK39 or EDN2 and TBK1 is more effective than concurrent depletion in sensitizing ovarian cancer cell lines to paclitaxel and in stabilizing microtubules.** To validate results with pooled siRNAs for the two most active combinations, we first tested the knockdown efficiency of 4 individual siRNA oligomers (**Figure S2A-D**), and then determined the  $IC_{50}$  of paclitaxel with and without siRNA treatment in the HeyA8, SKOV3ip and OVCAR5 ovarian cancer cell lines. Each of the 4 siRNAs (siIKBKB, siSTK39, siEDN2 and siTBK1) sensitized each cell line to paclitaxel (**Figure 2B-C**). Combined depletion of IKBKB/STK39 or EDN2/TBK1 had a greater effect in each case than knockdown of individual kinases (**Figure 2B-C**). Treatment with siIKBKB before siSTK39 or siEDN2 before siTBK1 produced a greater reduction in  $IC_{50}$  than treatment in the opposite order. Moreover, concurrent depletion of the kinases produced less sensitization to paclitaxel than sequential treatment in the optimal order.

Used sequentially and in the optimal order, depletion of IKBK/STK39 enhanced paclitaxel sensitivity 1.6- to 4.8-fold (**Figure 2B**) and depletion of EDN2/TBK1 enhanced paclitaxel sensitivity 4.8- to 11.4-fold (**Figure 2C**) across different ovarian cancer cell lines when compared to the IC<sub>50</sub> for paclitaxel of siRNA controls.

To determine the effect of dual kinase depletion on microtubule stability, we measured expression of glu-tubulin and quantified the microtubule and free-tubulin cellular fractions in HeyA8 and OVCAR5 cell lines to determine whether the effect of cell viability by siIKBKB/siSTK39 or siEDN2/siTBK1 treatment was inversely correlated with microtubule stability. We discovered that the sequential transfection of siIKBKB followed by siSTK39 (siIKBKB-siSTK39) induced a greater stabilizing effect than 1) either single siRNA, 2) combinations in a reversed order (siSTK39-siIKBKB), or 3) simultaneous transfection of both siRNA in each of two ovarian cancer cell lines (**Figure 3A, S3A, S4A and S4E**). Similar results were also observed using EDN2 and TBK1 dual siRNA in each of two ovarian cancer cell lines (**Figure 3B, S3B, S4B, and S4F**). Enhanced microtubule stability correlated with enhanced sensitization to paclitaxel, consistent with the possibility that sequence dependent depletion of IKBK/STK39 or EDN2/TBK1 modulate paclitaxel sensitivity by regulating microtubule stability.

**Increasing microtubule stability and paclitaxel sensitivity by depletion of IKBKB and STK39 or EDN2 and TBK1 is dependent upon p38-mediated phosphorylation of MAP4.** To examine underlying mechanism(s) by which depletion of pairs of kinases enhances microtubule stability, we first tested whether p38 signalling is involved in kinase-induced phosphorylation of microtubule-associated protein-4 (MAP4) in ovarian cancer cells. HeyA8 or OVCAR5 cells were reverse transfected with siControl or siIKBKB / siSTK39 or siEDN2 / siTBK1 for 24 hrs. Activities of p38 and MAP4 were assessed using Western blot analysis with a phospho-specific p38 antibody (Thr180/Tyr182) and a phospho-specific MAP4 antibody (Ser696), respectively. The activity of p38 and MAP4 was significantly decreased after depletion of IKBKB/STK39 or EDN2/TBK1 (**Figure 3C-D and S3C-D**). We next tested whether p38 / MAP4 signaling was essential for IKBKB/STK39- or EDN2/TBK1-induced enhancement of microtubule stability in ovarian cancer cells. Microtubule stabilities were measured in HeyA8 or OVCAR5 cells by transfecting of siMAP4 and siIKBKB / siSTK39 or siEDN2 / siTBK1 for 72 hrs. Knockdown of MAP4 using MAP4 siRNA partially blocked dual siRNA induced enhancement of microtubule stability (**Figure 3E-F, S3E-F, S4C-D and S4E-F**) and decreased dual siRNA induced paclitaxel sensitization when compared to the IC<sub>50</sub> for paclitaxel of siIKBKB/siSTK39 or siEDN2/siTBK1 (**Figure S5**). These results indicate that IKBKB/STK39 or EDN2/TBK1 act upstream to promote p38 activation-mediated MAP4 phosphorylation and to decrease microtubule stability as well as paclitaxel sensitivity in ovarian cancer.

**Sequential depletion of IKBKB/STK39 or EDN2/TBK1 enhances paclitaxel induced-apoptosis and cell cycle arrest.** To delineate the mechanism(s) involved in the effect of dual kinase depletion on paclitaxel-induced growth inhibition and cell death in ovarian cancer, SKOV3ip, HeyA8 and OVCAR5 cell lines were treated with two siRNAs sequentially or simultaneously followed by paclitaxel treatment as described above. Apoptosis was measured with Annexin V using flow cytometry. Sequential depletion of IKBKB/STK39 or EDN2/TBK1 greatly enhanced paclitaxel-induced apoptosis compared to depletion of the individual kinases or depletion by sequential siRNA transfection in reverse order, or simultaneous transfection of both

siRNAs (**Figure 4A and 4C**). Importantly, these data confirm our previous observations with an SRB assay that sequential depletion of IKBKB/STK39 or EDN2/TBK1 enhances paclitaxel-mediated growth inhibition. To determine whether dual kinase depletion affects cell cycle kinetics or modulates paclitaxel-induced G2/M cell cycle arrest (24), we performed cell cycle analysis and observed a slight but significant G2/M arrest in SKOV3ip, HeyA8 and OVCAR5 cells with single kinase knockdown and a more dramatic mitotic block in the cells sequentially transfected with dual siRNA (siIKBKB/siSTK39) which was consistent with the induction of apoptosis, however siEDN2/siTBK1 induced G1 arrest and did not increase paclitaxel-mediated G2/M arrest, although significant induction of apoptosis was observed (**Figure 4B and 4D**). Taken together, our data suggest that sequential kinase depletion promotes cell cycle arrest and paclitaxel induced apoptosis by enhancing microtubule stability.

**Depletion of IKBKB/STK39 and EDN2/TBK1 sensitize human ovarian cancer xenografts to paclitaxel.** To test whether studies with human ovarian cancer cells in culture would translate to human ovarian cancers growing in vivo, we examined whether depletion of IKBKB/STK39 or EDN2/TBK1 significantly enhanced paclitaxel sensitivity in human ovarian cancer xenografts in nu/nu mice using the well-characterized DOPC (1,2-dioleoyl-sn-glycero-3-phosphatidylcholine) nanoliposomal delivery system (11). For each cancer cell line, 8 groups of 10 mice were treated for 4 weeks as follows: 1) control siRNA-DOPC, 2) control siRNA-DOPC plus paclitaxel, 3) IKBKB (or EDN2) siRNA-DOPC, 4) IKBKB (or EDN2) siRNA-DOPC plus paclitaxel, 5) STK39 (or TBK1) siRNA-DOPC, 6) STK39 (or TBK1) siRNA-DOPC plus paclitaxel 7) IKBKB/STK39 (or EDN2/TBK1) siRNA-DOPC, 8) IKBKB/STK39 (or EDN2/TBK1) siRNA-DOPC plus paclitaxel. The combination of IKBKB/STK39 siRNAs with paclitaxel had a greater effect on tumor growth than any other group and exerted statistically significant inhibition of xenograft growth when compared to paclitaxel alone in SKOV3ip ( $p=0.0172$ ) and OVCAR5 ( $p=0.0078$ ) xenograft models (**Figure 5A**), however mice treated with dual siRNAs plus paclitaxel showed no sign of toxicity as evidenced by no significant weight loss compared to control mice after 5-week treatment (**Figure S6A**). The combination of EDN2 and TBK1 with paclitaxel produced a similar trend in growth inhibition using SKOV3ip ovarian cancer model where significant inhibition ( $P=0.0471$ ) was observed only with the combined treatment (**Figure 5B and S6B**). Together, these data confirm that depletion of IKBKB/STK39 or EDN2/TBK1 inhibits human ovarian cancer cell growth and enhances paclitaxel sensitivity not only in cultured cells, but also in ovarian cancer xenografts.

**IKBKB and STK39 are overexpressed in ovarian cancer and are associated with poor prognosis.** Translation of these observations to the clinic will depend upon the expression of the relevant kinases in human ovarian cancers. We have measured the expression of IKBKB and STK39 in ovarian cancer patient specimens. Immunohistochemical analysis was performed with an ovarian cancer tissue microarray (TMA) staining for IKBKB and STK39 was quantitated on a scale of 0 to 3 for the intensity of the expression, with 0 to 1 being negative and 2 to 3 being positive (**Figure 6A**). When compared to immunostaining of normal ovarian surface epithelial cells, overexpression of IKBKB and STK39 was observed in 54% and 56% of ovarian cancers, respectively (**Figure 6B and Table S8**). Upregulation of both IKBKB and STK39 proteins correlated with a poor prognosis. Overexpression of IKBKB was associated with a decrease in overall survival of 13 months, overexpression of STK39 with 11.3 months poorer survival and overexpression of both kinases with a decrease of 19 months (**Figure 6C and Table S8**).

Consequently, targeted siRNA therapy could benefit patients with overexpression of IKBKB, STK39 or both.

## DISCUSSION

Primary resistance to paclitaxel is a major obstacle to successful treatment of ovarian cancer. Our study suggests that knockdown of 4 kinases can enhance sensitivity to paclitaxel by stabilizing microtubules and that dual kinase knockdown is more effective than silencing individual kinases. To enhance the efficacy of paclitaxel and provide a rationale for siRNA based therapy for ovarian cancer, we selected 14 candidates from a previous kinome screen that enhanced paclitaxel sensitivity (11) and validated these targets in 12 ovarian cancer cell lines with different molecular characteristics. We discovered that dual silencing of IKBKB/STK39 or EDN2/TBK1 enhanced paclitaxel sensitivity by stabilizing microtubules through downregulation of p38 mediated phosphorylation of MAP4 that enhanced paclitaxel-induced apoptosis and arrested the cell cycle. We confirmed that the combination of IKBKB/STK39 and EDN2/TBK1 siRNAs enhanced paclitaxel sensitivity in two ovarian cancer xenograft models.

Microtubule dynamics in cells relies in part on the intrinsic properties of  $\alpha$ - $\beta$ -tubulin dimer and its ability to bind and hydrolyze a GTP nucleotide (25). The tubulin dimer is subject to special posttranslational modifications such as glutamylation, tyrosination, and acetylation (26). Microtubule dynamics are also regulated by a number of microtubule effectors, including microtubule-associated proteins (MAPs), molecular motors such as kinesins, the Ras-like GTPase Ran-GTP, microtubule plus end-directed proteins and tubulin-binding proteins (27). These microtubule- or tubulin-associated proteins are themselves under the control of a balance of protein phosphatases and kinases. In our current study, stabilization of microtubules and sensitization to paclitaxel were achieved by knockdown of each of 4 kinases that regulate p38-mediated phosphorylation of a common microtubule-associated protein, MAP4. Phosphorylation of the microtubule associated protein CRMP2 by FIR (9) and phosphorylation of MAP4 and MAP1B by SYK (28) have also been shown to modulate microtubule stability and paclitaxel sensitivity.

Activation of p38 previously has been reported to lead to MAP4 phosphorylation, inducing microtubule destabilization (29). MAP4 is thought to affect microtubule dynamics by stabilizing the microtubule lattice (30). Phosphorylation of MAP4 disrupts this stabilization (30). We have found that down regulation of IKBKB/STK59 or EDN2/TBK1 decreases phosphorylation of MAP4 after phosphor-p38 inhibition, stabilizing microtubules. Paclitaxel is a microtubule stabilizing drug and paclitaxel binds to specific pockets with  $\beta$  tubulin in  $\alpha/\beta$  tubulin dimers increasing microtubule polymerization and stability (31). While phosphorylation of MAP4 could reduce the microtubule-stabilizing potency of Taxol (32), inhibition of MAP4 phosphorylation could augment paclitaxel's activity.

Modulating the NF $\kappa$ B pathway could aid in more effective cancer therapy. Through the canonical pathway, IKBKB, phosphorylates I $\kappa$ B, the inhibitor of the NF $\kappa$ B complex. I $\kappa$ B phosphorylation leads to proteasomal degradation, freeing the NF $\kappa$ B complex (33). The p65 (RelA) subunit of NF $\kappa$ B is then translocated into nucleus and initiates transcription of a number of anti-apoptotic

genes including TRAF-1, BCL2, BCL2L1 and the IAPs (34,35). NFκB activation has been observed in epithelial ovarian cancer. p65 (RelA) has been detected in 75% of ovarian cancer cases, compared to 27% of normal ovaries (36). STK39, Serine threonine kinase 39 (STK39), encoding a STE20/SPS1-related proline/alanine-rich kinase (SPAK), has been implicated association with several biological roles including cell differentiation (37), cell transformation (38), proliferation and cytoskeleton rearrangement (39). NFκB transcriptionally regulates the expression of STK39 gene by directly binding to the promoter of the STK39 or altering chromatin, recruiting transcription initiation machinery and enhancing peptide the elongation (40). More importantly, a linkage has been established between STK39 and the p38 pathway (41). Thus, the role of both STK39 and IKBKB to affect the NFκB signaling pathway and downstream p38 supports the results that dual kinase inhibition increases paclitaxel sensitivity in ovarian cancers.

Sequential administration of siRNAs against IKBKB before STK39 was more effective in enhancing paclitaxel activity than simultaneous treatment with both siRNAs or sequential treatment in the reverse order *in vitro*. As NFκB induces anti-apoptotic proteins, time would be required for these to be depleted prior to the initiation of apoptosis through inhibition of the p38 pathway by STK39 depletion, as well as through the enhanced paclitaxel activity produced by stabilization of microtubules by decreased phosphorylation of MAP4 after p38 inhibition. For a clinical approach, as one could expect, there is a time dependent mechanism that one agent may simply reinforce the action of another agent in cancer treatment (e.g. sequential days of treatment). For example, treatment with a potent inhibitor of IKBKB and then followed with staggered targeted inhibition of STK39. Similarly, inhibition of EDN2 would then be followed by inhibition of TBK1. To confirm this hypothesis, animal models would need to be obtained and treated in a similar fashion once small molecules or other targeted therapies become available before this could be implemented in the clinical setting. In addition, depending on their pharmacokinetics and pharmacodynamics, sequential therapy may allow the optimal delivery of single-drug therapy and potentially reduces the risk of toxicity, which may improve quality of life

In our current study, overexpression of IKBKB and STK39 was documented in 54% and 56% of ovarian cancers, respectively. Upregulation of both IKBKB and STK39 proteins correlated with a poor prognosis and depletion of IKBKB/STK39 sensitizes ovarian cancer to paclitaxel by decreasing activity of p38 and MAP4 and enhancing microtubule stability. Thus, our data suggest that IKBKB/STK39 play an important role in oncogenic kinase-mediated tumor cell proliferation and chemoresistance through the NFκB/STK39/p38/MAP4 signaling pathway. Targeted siRNA therapy could benefit ovarian cancer patients with overexpression of IKBKB, STK39 or both.

The function of EDN2 is not well understood, although it has been implicated as protective of photoreceptor loss in mice predisposed to retinopathy (42). EDN2 (ET-2) differs from EDN1 (ET-1) by only two amino acids (43). It was considered that EDN2 would mimic the actions of EDN1 and current pharmacological interventions used to inhibit the EDN1 system would also block the actions of EDN2 (44). However, recent research suggests that although EDN2 is very similar in structure to EDN1, EDN2 has been shown to regulate cancer cell apoptosis and affect invasion and metastasis in breast cancer (45). EDN1-induced cell proliferation occurs primarily via its activation of the p38 signaling pathway (46). To our knowledge there has not been a prior report describing the role of EDN2 regulation of p38. Once again, siRNA therapy targeting EDN2 could be tested clinically if efficient delivery can be achieved.

TBK1, a non-canonical IKK, is activated by TLR3 and TLR4 signaling and functions together with IKK $\epsilon$  as an intermediate in the activation of the transcription factor IRF3. Activated IKK $\epsilon$  subsequently translocates into the nucleus and induces expression of IRF3-dependent genes (47). There can be significant crosstalk between the NF $\kappa$ B-p62 (canonical) and IRF3 (non-canonical) pathways. NF $\kappa$ B can bind to the 5' promoter region of the EDN1 gene. Overexpression of the cytoplasmic inhibitor of NF $\kappa$ B or deletion of the NF $\kappa$ B binding site reduced EDN1 induction, whereas overexpression of NF $\kappa$ B p65 induced EDN1 (48), but there is no report indicating that NF $\kappa$ B signaling induces EDN2 expression. BX795 was the first TBK1 inhibitor to be patented (49). The JAK1 and JAK2 inhibitor momelotinib (CYT387) is also a potent inhibitor of TBK1 (50). Future studies can evaluate these drugs individually and in combination to potentiate paclitaxel sensitivity.

## ACKNOWLEDGEMENTS

This work was supported by the Cancer Prevention and Research Institute of Texas RP110595-P1, the MD Anderson SPORE in Ovarian Cancer NCI P50 CA 83639, the Shared Resources of the MD Anderson CCSG grant NCI P30 CA16672, R35 CA209904, the American Cancer Society Research Professor Award, the Frank McGraw Memorial Chair in Cancer Research, The National Foundation for Cancer Research, the philanthropic support from generous donations from Stuart and Gaye-Lynn Zarrow, the Mossy foundation and the Roberson endowment. AA is supported by grants from the NIHR National Institute for Health Research (NIHR) Oxford Biomedical Research Centre (BRC) and Ovarian Cancer Action.

## REFERENCES

1. Kurman RJ, Shih Ie M. The Dualistic Model of Ovarian Carcinogenesis: Revisited, Revised, and Expanded. *Am J Pathol* **2016**;186(4):733-47 doi 10.1016/j.ajpath.2015.11.011.
2. Muggia FM. Sequential single agents as first-line chemotherapy for ovarian cancer: a strategy derived from the results of GOG-132. *Int J Gynecol Cancer* **2003**;13 Suppl 2:156-62.
3. Parmar MK, Ledermann JA, Colombo N, du Bois A, Delaloye JF, Kristensen GB, *et al.* Paclitaxel plus platinum-based chemotherapy versus conventional platinum-based chemotherapy in women with relapsed ovarian cancer: the ICON4/AGO-OVAR-2.2 trial. *Lancet* **2003**;361(9375):2099-106.
4. McGrogan B, Phelan S, Fitzpatrick P, Maguire A, Prencipe M, Brennan D, *et al.* Spindle assembly checkpoint protein expression correlates with cellular proliferation and shorter time to recurrence in ovarian cancer. *Hum Pathol* **2014**;45(7):1509-19 doi 10.1016/j.humpath.2014.03.004.
5. Horwitz SB. Taxol (paclitaxel): mechanisms of action. *Ann Oncol* **1994**;5 Suppl 6:S3-6.
6. Cabral F, Abraham I, Gottesman MM. Isolation of a taxol-resistant Chinese hamster ovary cell mutant that has an alteration in alpha-tubulin. *Proc Natl Acad Sci U S A* **1981**;78(7):4388-91.
7. Ahmed AA, Mills AD, Ibrahim AE, Temple J, Blenkinsop C, Vias M, *et al.* The extracellular matrix protein TGFBI induces microtubule stabilization and sensitizes ovarian cancers to paclitaxel. *Cancer Cell* **2007**;12(6):514-27 doi 10.1016/j.ccr.2007.11.014.
8. Ahmed AA, Wang X, Lu Z, Goldsmith J, Le XF, Grandjean G, *et al.* Modulating microtubule stability enhances the cytotoxic response of cancer cells to Paclitaxel. *Cancer Res* **2011**;71(17):5806-17 doi 10.1158/0008-5472.CAN-11-0025.



9. Zheng Y, Sethi R, Mangala LS, Taylor C, Goldsmith J, Wang M, *et al.* Tuning microtubule dynamics to enhance cancer therapy by modulating FER-mediated CRMP2 phosphorylation. *Nat Commun* **2018**;9(1):476 doi 10.1038/s41467-017-02811-7.
10. Shi X, Sun X. Regulation of paclitaxel activity by microtubule-associated proteins in cancer chemotherapy. *Cancer Chemother Pharmacol* **2017** doi 10.1007/s00280-017-3398-2.
11. Ahmed AA, Lu Z, Jennings NB, Etemadmoghadam D, Capalbo L, Jacamo RO, *et al.* SIK2 is a centrosome kinase required for bipolar mitotic spindle formation that provides a potential target for therapy in ovarian cancer. *Cancer Cell* **2010**;18(2):109-21 doi 10.1016/j.ccr.2010.06.018.
12. Kazemi-Oula G, Ghafouri-Fard S, Mobasheri MB, Geranpayeh L, Modarressi MH. Upregulation of RHOXF2 and ODF4 Expression in Breast Cancer Tissues. *Cell J* **2015**;17(3):471-7.
13. Zhou H, Wertz I, O'Rourke K, Ultsch M, Seshagiri S, Eby M, *et al.* Bcl10 activates the NF-kappaB pathway through ubiquitination of NEMO. *Nature* **2004**;427(6970):167-71 doi 10.1038/nature02273.
14. Wang R, Lohr CV, Fischer K, Dashwood WM, Greenwood JA, Ho E, *et al.* Epigenetic inactivation of endothelin-2 and endothelin-3 in colon cancer. *Int J Cancer* **2013**;132(5):1004-12 doi 10.1002/ijc.27762.
15. Tetreault MP, Weinblatt D, Ciolino JD, Klein-Szanto AJ, Sackey BK, Twyman-Saint Victor C, *et al.* Esophageal Expression of Active IkappaB Kinase-beta in Mice Up-Regulates Tumor Necrosis Factor and Granulocyte-Macrophage Colony-Stimulating Factor, Promoting Inflammation and Angiogenesis. *Gastroenterology* **2016**;150(7):1609-19 e11 doi 10.1053/j.gastro.2016.02.025.
16. Chen D, Zhang Y, Zhang X, Li J, Han B, Liu S, *et al.* Overexpression of integrin-linked kinase correlates with malignant phenotype in non-small cell lung cancer and promotes lung cancer cell invasion and migration via regulating epithelial-mesenchymal transition (EMT)-related genes. *Acta Histochem* **2013**;115(2):128-36 doi 10.1016/j.acthis.2012.05.004.
17. Cordes N. Overexpression of hyperactive integrin-linked kinase leads to increased cellular radiosensitivity. *Cancer Res* **2004**;64(16):5683-92 doi 10.1158/0008-5472.CAN-04-1056.
18. Shen FF, Yue WB, Zhou FY, Pan Y, Zhao XK, Jin Y, *et al.* Variations in the MHC region confer risk to esophageal squamous cell carcinoma on the subjects from high-incidence area in northern China. *PLoS One* **2014**;9(3):e90438 doi 10.1371/journal.pone.0090438.
19. Bon H, Wadhwa K, Schreiner A, Osborne M, Carroll T, Ramos-Montoya A, *et al.* Salt-inducible kinase 2 regulates mitotic progression and transcription in prostate cancer. *Mol Cancer Res* **2015**;13(4):620-35 doi 10.1158/1541-7786.MCR-13-0182-T.
20. Miranda F, Mannion D, Liu S, Zheng Y, Mangala LS, Redondo C, *et al.* Salt-Inducible Kinase 2 Couples Ovarian Cancer Cell Metabolism with Survival at the Adipocyte-Rich Metastatic Niche. *Cancer Cell* **2016**;30(2):273-89 doi 10.1016/j.ccell.2016.06.020.
21. Hendriksen PJ, Dits NF, Kokame K, Veldhoven A, van Weerden WM, Bangma CH, *et al.* Evolution of the androgen receptor pathway during progression of prostate cancer. *Cancer Res* **2006**;66(10):5012-20 doi 10.1158/0008-5472.CAN-05-3082.
22. Li Z, Zhu W, Xiong L, Yu X, Chen X, Lin Q. Role of high expression levels of STK39 in the growth, migration and invasion of non-small cell type lung cancer cells. *Oncotarget* **2016**;7(38):61366-77 doi 10.18632/oncotarget.11351.
23. Townley HE, Zheng Y, Goldsmith J, Zheng YY, Stratford MR, Dobson PJ, *et al.* A novel biosensor for quantitative monitoring of on-target activity of paclitaxel. *Nanoscale* **2015**;7(3):1127-35 doi 10.1039/c4nr01105h.
24. Choi YH, Yoo YH. Taxol-induced growth arrest and apoptosis is associated with the upregulation of the Cdk inhibitor, p21WAF1/CIP1, in human breast cancer cells. *Oncol Rep* **2012**;28(6):2163-9 doi 10.3892/or.2012.2060.
25. Mitchison T, Kirschner M. Dynamic instability of microtubule growth. *Nature* **1984**;312(5991):237-42.

26. Westermann S, Weber K. Post-translational modifications regulate microtubule function. *Nat Rev Mol Cell Biol* **2003**;4(12):938-47 doi 10.1038/nrm1260.
27. Galjart N, Perez F. A plus-end raft to control microtubule dynamics and function. *Curr Opin Cell Biol* **2003**;15(1):48-53.
28. Yu Y, Gaillard S, Phillip JM, Huang TC, Pinto SM, Tessarollo NG, *et al.* Inhibition of Spleen Tyrosine Kinase Potentiates Paclitaxel-Induced Cytotoxicity in Ovarian Cancer Cells by Stabilizing Microtubules. *Cancer Cell* **2015**;28(1):82-96 doi 10.1016/j.ccell.2015.05.009.
29. Hu JY, Chu ZG, Han J, Dang YM, Yan H, Zhang Q, *et al.* The p38/MAPK pathway regulates microtubule polymerization through phosphorylation of MAP4 and Op18 in hypoxic cells. *Cell Mol Life Sci* **2010**;67(2):321-33 doi 10.1007/s00018-009-0187-z.
30. Illenberger S, Drewes G, Trinczek B, Biernat J, Meyer HE, Olmsted JB, *et al.* Phosphorylation of microtubule-associated proteins MAP2 and MAP4 by the protein kinase p110mark. Phosphorylation sites and regulation of microtubule dynamics. *J Biol Chem* **1996**;271(18):10834-43.
31. Nogales E, Wolf SG, Khan IA, Luduena RF, Downing KH. Structure of tubulin at 6.5 Å and location of the taxol-binding site. *Nature* **1995**;375(6530):424-7 doi 10.1038/375424a0.
32. Orr GA, Verdier-Pinard P, McDaid H, Horwitz SB. Mechanisms of Taxol resistance related to microtubules. *Oncogene* **2003**;22(47):7280-95 doi 10.1038/sj.onc.1206934.
33. Lawrence T. The nuclear factor NF-kappaB pathway in inflammation. *Cold Spring Harb Perspect Biol* **2009**;1(6):a001651 doi 10.1101/cshperspect.a001651.
34. Napetschnig J, Wu H. Molecular basis of NF-kappaB signaling. *Annu Rev Biophys* **2013**;42:443-68 doi 10.1146/annurev-biophys-083012-130338.
35. Facchini FS, Humphreys MH, DoNascimento CA, Abbasi F, Reaven GM. Relation between insulin resistance and plasma concentrations of lipid hydroperoxides, carotenoids, and tocopherols. *Am J Clin Nutr* **2000**;72(3):776-9.
36. Guo RX, Qiao YH, Zhou Y, Li LX, Shi HR, Chen KS. Increased staining for phosphorylated AKT and nuclear factor-kappaB p65 and their relationship with prognosis in epithelial ovarian cancer. *Pathol Int* **2008**;58(12):749-56 doi 10.1111/j.1440-1827.2008.02306.x.
37. Dan I, Watanabe NM, Kusumi A. The Ste20 group kinases as regulators of MAP kinase cascades. *Trends Cell Biol* **2001**;11(5):220-30.
38. Dowd BF, Forbush B. PASK (proline-alanine-rich STE20-related kinase), a regulatory kinase of the Na-K-Cl cotransporter (NKCC1). *J Biol Chem* **2003**;278(30):27347-53 doi 10.1074/jbc.M301899200.
39. Li Y, Hu J, Vita R, Sun B, Tabata H, Altman A. SPAK kinase is a substrate and target of PKCtheta in T-cell receptor-induced AP-1 activation pathway. *EMBO J* **2004**;23(5):1112-22 doi 10.1038/sj.emboj.7600125.
40. Yan Y, Dalmasso G, Nguyen HT, Obertone TS, Charrier-Hisamuddin L, Sitaraman SV, *et al.* Nuclear factor-kappaB is a critical mediator of Ste20-like proline-/alanine-rich kinase regulation in intestinal inflammation. *Am J Pathol* **2008**;173(4):1013-28 doi 10.2353/ajpath.2008.080339.
41. Johnston AM, Naselli G, Gonez LJ, Martin RM, Harrison LC, DeAizpurua HJ. SPAK, a STE20/SPS1-related kinase that activates the p38 pathway. *Oncogene* **2000**;19(37):4290-7 doi 10.1038/sj.onc.1203784.
42. Samardzija M, Wariwoda H, Imsand C, Huber P, Heynen SR, Gubler A, *et al.* Activation of survival pathways in the degenerating retina of rd10 mice. *Exp Eye Res* **2012**;99:17-26 doi 10.1016/j.exer.2012.04.004.
43. Wang Y, O'Connell JR, McArdle PF, Wade JB, Dorff SE, Shah SJ, *et al.* From the Cover: Whole-genome association study identifies STK39 as a hypertension susceptibility gene. *Proc Natl Acad Sci U S A* **2009**;106(1):226-31 doi 10.1073/pnas.0808358106.
44. Sethi G, Sung B, Kunnumakkara AB, Aggarwal BB. Targeting TNF for Treatment of Cancer and Autoimmunity. *Adv Exp Med Biol* **2009**;647:37-51 doi 10.1007/978-0-387-89520-8\_3.

45. Karin M, Cao Y, Greten FR, Li ZW. NF-kappaB in cancer: from innocent bystander to major culprit. *Nat Rev Cancer* **2002**;2(4):301-10 doi 10.1038/nrc780.
46. Muller E, Burger-Kentischer A, Neuhofer W, Fraek ML, Marz J, Thureau K, *et al.* Possible involvement of heat shock protein 25 in the angiotensin II-induced glomerular mesangial cell contraction via p38 MAP kinase. *J Cell Physiol* **1999**;181(3):462-9 doi 10.1002/(SICI)1097-4652(199912)181:3<462::AID-JCP10>3.0.CO;2-T.
47. Shen RR, Hahn WC. Emerging roles for the non-canonical IKKs in cancer. *Oncogene* **2011**;30(6):631-41 doi 10.1038/ncr.2010.493.
48. Quehenberger P, Bierhaus A, Fasching P, Muellner C, Klevesath M, Hong M, *et al.* Endothelin 1 transcription is controlled by nuclear factor-kappaB in AGE-stimulated cultured endothelial cells. *Diabetes* **2000**;49(9):1561-70.
49. Yu T, Yang Y, Yin DQ, Hong S, Son YJ, Kim JH, *et al.* TBK1 inhibitors: a review of patent literature (2011 - 2014). *Expert Opin Ther Pat* **2015**;25(12):1385-96 doi 10.1517/13543776.2015.1081168.
50. Pardnani A, Lasho T, Smith G, Burns CJ, Fantino E, Tefferi A. CYT387, a selective JAK1/JAK2 inhibitor: in vitro assessment of kinase selectivity and preclinical studies using cell lines and primary cells from polycythemia vera patients. *Leukemia* **2009**;23(8):1441-5 doi 10.1038/leu.2009.50.

## Figure Legends

**Figure 1. Effects of single kinase siRNA on microtubule stability.** (A) siEDN2, siIKKB, siSIK2 and siSTK39 treatment enhanced microtubule stability in the SKOV3ip cell line. Cells were reversely transfected with kinase siRNA (siGENOME SMARTpool) for 48 hrs and lysed. Duplicate samples were loaded and immunoblots were performed with specific antibodies as indicated. (B) Treatment of other Kinase siRNAs exhibited little or no changes in microtubule stability. Cell treatment was carried out as described above. (C) The quantification of the band intensity for western blotting of (A) and (B). (D) siRNA knockdown efficiency was calculated using quantitation of mRNA. The columns indicate the mean  $\pm$  S.D. (\*  $p < 0.05$  and \*\*  $p < 0.01$  compared to paired siControl). Data were obtained from two independent experiments.

**Figure 2. Sequential treatment with siIKKB followed by siSTK39 or with siEDN2 followed by siTBK1 enhances paclitaxel sensitivity in ovarian cancer cells.** (A) A supervised heatmap represents medium-centered fold change of paclitaxel sensitivity after dual siRNA treatment. A2780, CaOv3, EFO21, HeyA8, OAW42 and SKOV3ip ovarian cancer -cells were treated with dual siRNA sequentially followed by paclitaxel treatment, and then cells were stained using SRB assay. A -hHeatmap was generated using median-centered fold changes of paclitaxel sensitivity. The fold changes of each kinase siRNA were calculated using the ratio of the SRB assay value normalized to that of control siRNA, with and without paclitaxel treatment. A heat map generated from normalized fold changes displays the differences of the z-scores. (B) Combination of IKKB and STK39 treatment was examined in SKOV3ip, HeyA8 and OVCAR5 cell lines. Cells were treated with dual siRNA followed by addition of paclitaxel for 72 hrs. Cell growth was examined using an SRB assay. Cell mass was reflected by absorbance at 570 nm and the percentage of paclitaxel-induced growth inhibition was calculated for each target siRNA relative to control

siRNA. Dose response curves were generated using non-linear regression with the Least Squares fitting method (GraphPad). IC<sub>50</sub> of paclitaxel and fold changes of IC<sub>50</sub> were calculated. **(C)** Combination of EDN2 and TBK1 was tested in SKOV3ip and HeyA8 cell lines. Cell treatments and growth curve plotting were conducted as described above. Data were obtained from three independent experiments. \*  $p < 0.05$  and \*\*  $p < 0.01$  compared to siControl; #  $p < 0.05$  and ##  $p < 0.01$  compared to single siRNA against either IKBKB or EDN2; +  $p < 0.05$  and ++  $p < 0.01$  compared to single siRNA against either STK39 or TBK1.

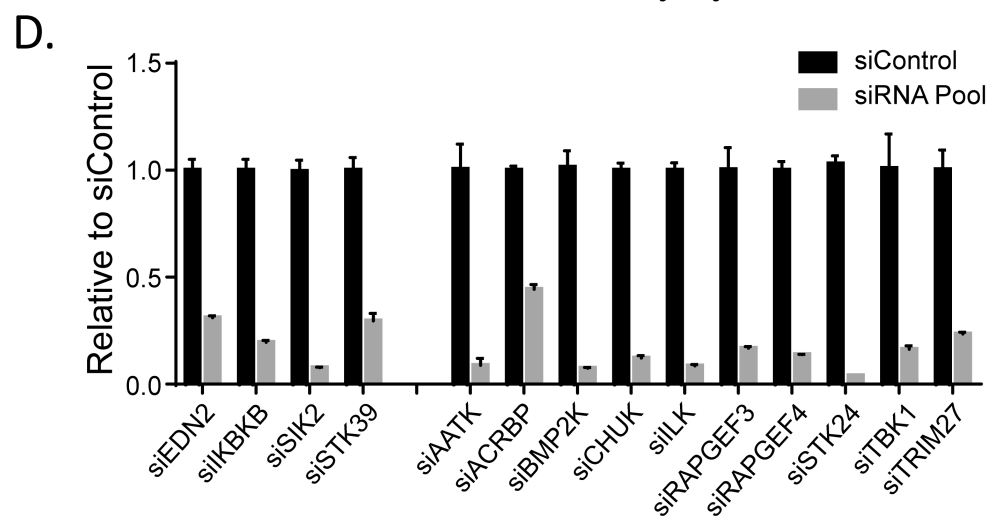
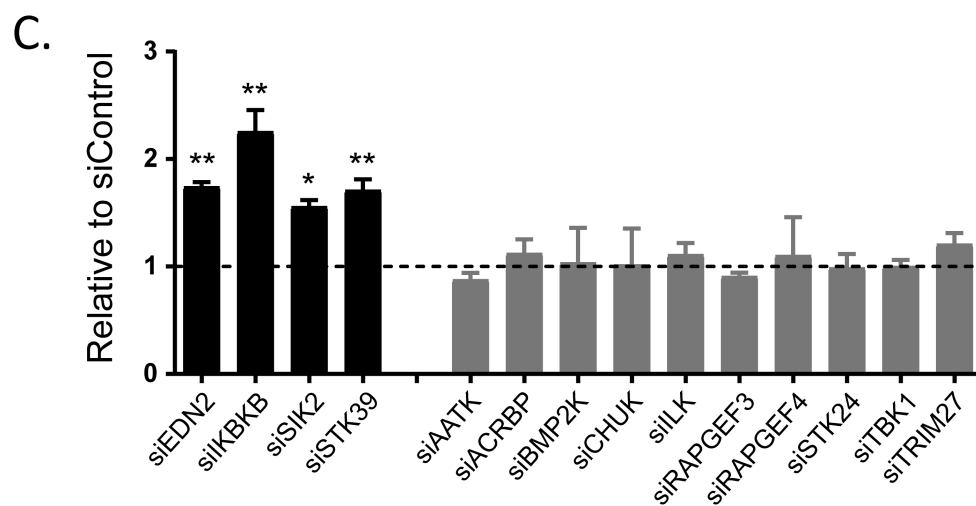
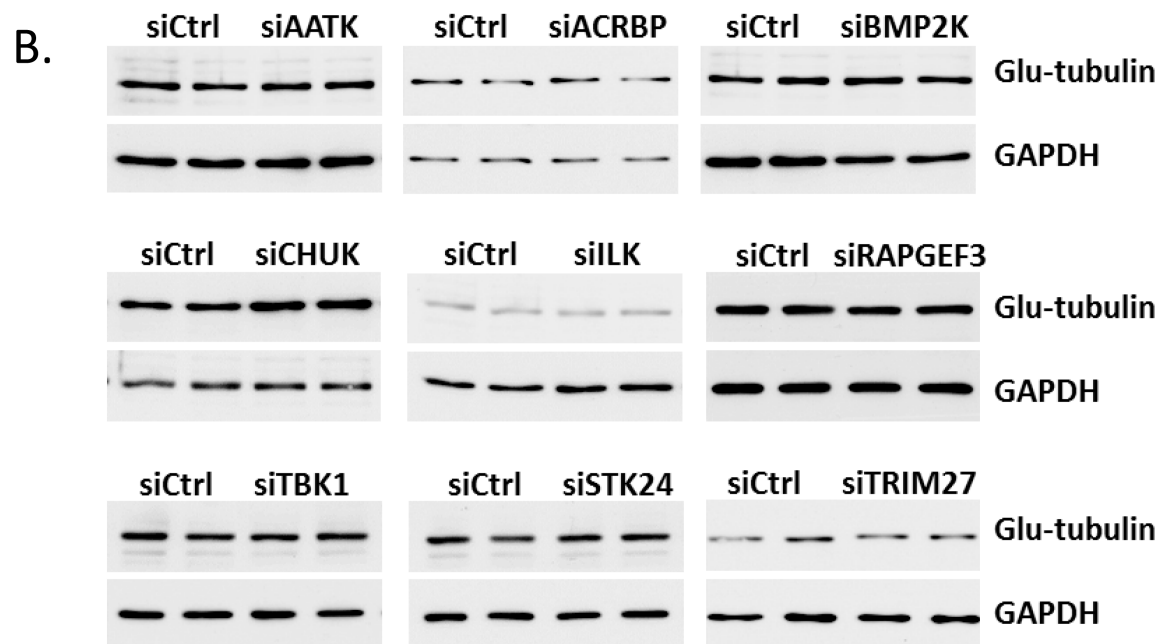
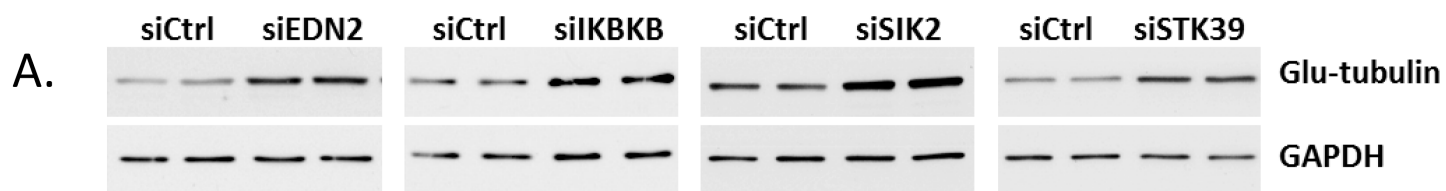
**Figure 3. Increasing microtubule stability by depletion of IKBKB and STK39 or EDN2 and TBK1 is dependent upon p38-mediated phosphorylation MAP4.** **(A-B)** Microtubule stability was examined in HeyA8 cells. Cells were treated with siIKBKB/siSTK39 or siEDN2/siTBK1 sequentially or simultaneously for 72 hrs. Cell lysates were collected and immunoblots were performed with specific antibodies as indicated. **(C-D)** p38-MAP4 signaling was examined in HeyA8 cells. Cells were treated with siIKBKB/siSTK39 or siEDN2/siTBK1 simultaneously for 24 hrs. Cell lysates were collected and immunoblots were performed with specific antibodies as indicated. **(E-F)** Microtubule stability was examined in HeyA8 cells. Cells were treated with siMAP4, siIKBKB and siSTK39 or siMAP4, siEDN2 and siTBK1 sequentially for 72 hrs. Immunoblots were carried out as described in (A). The columns indicate the mean, and the bars indicate the S.D. (\* $p < 0.05$  and \*\*  $p < 0.01$  compared with its own control). Data were obtained from three independent experiments. (C: Control; I: IKBKB; S: STK39; M: MAP4; E: EDN2; T: TBK1).

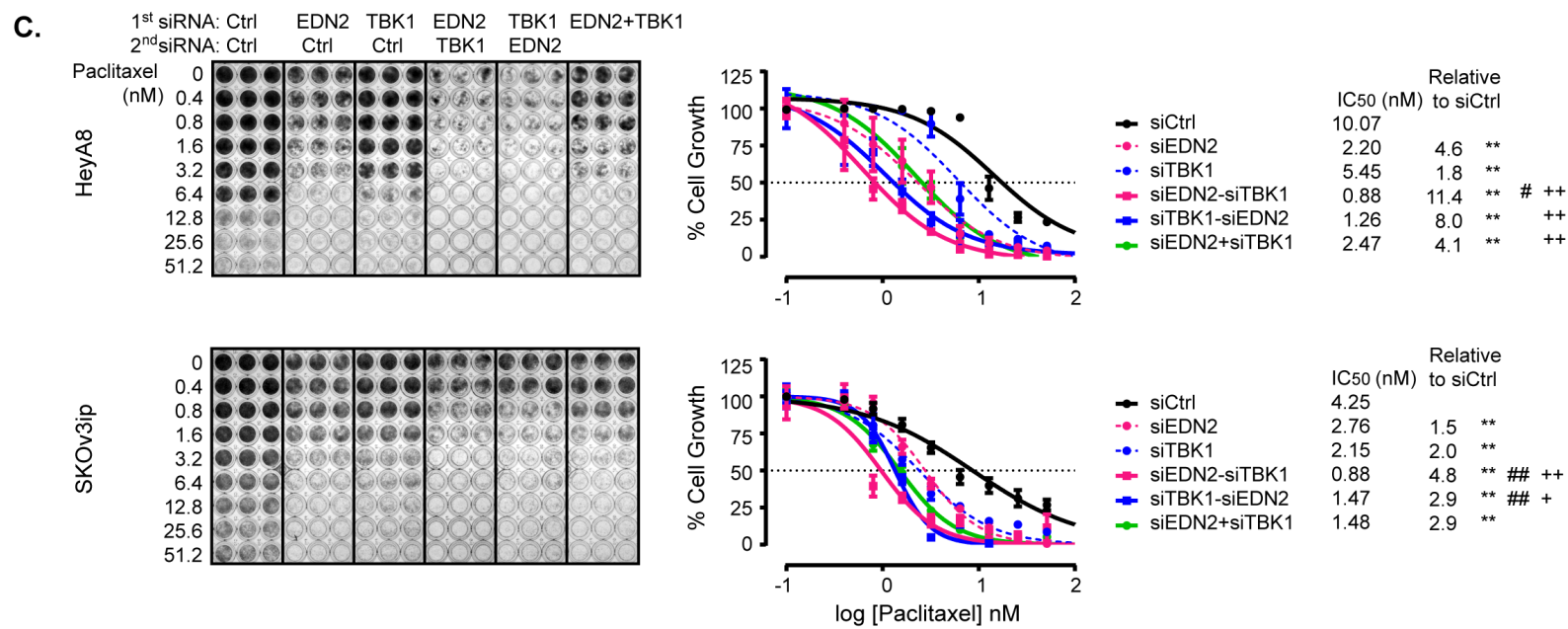
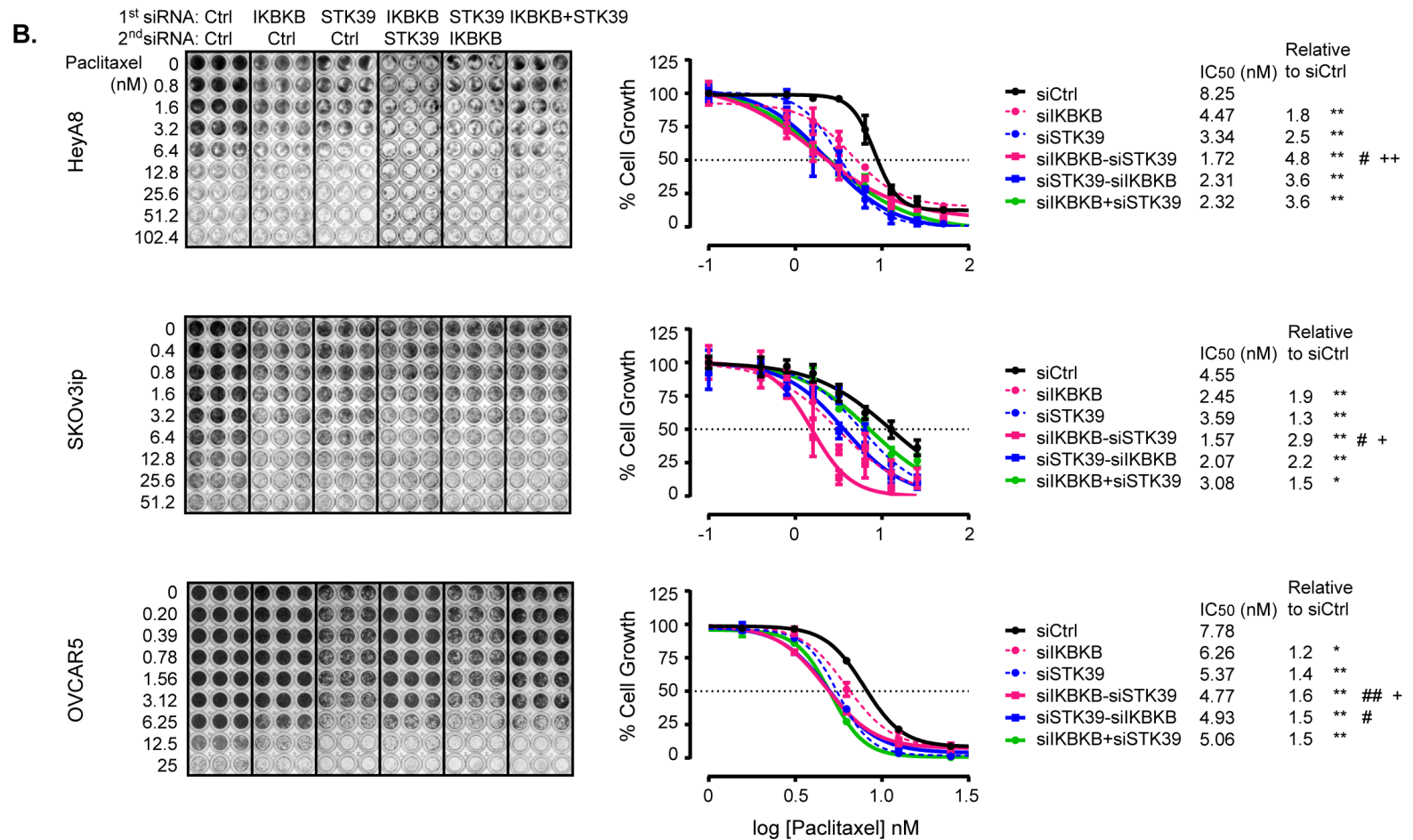
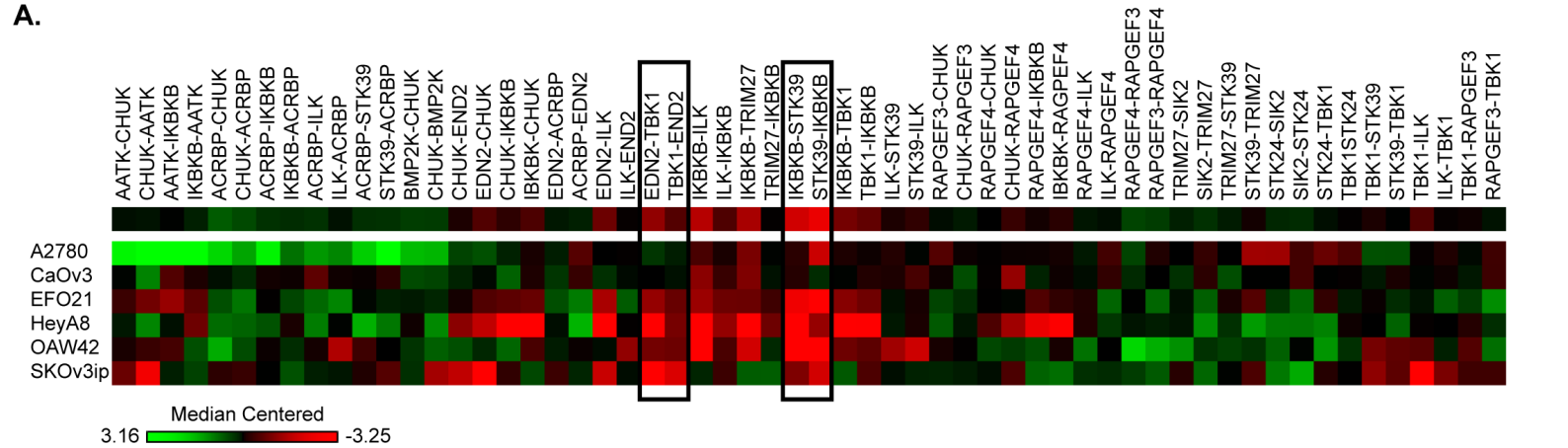
**Figure 4. Sequential treatment of siIKBKB followed by siSTK39 or siEDN2 followed by siTBK1 enhanced paclitaxel induced-apoptosis and G2/M cell cycle arrest.** **(A and C)** A combination of IKBKB and STK39 treatment was examined in SKOV3ip, HeyA8 and OVCAR5 cell lines. Cells were treated with dual siRNA followed by addition of paclitaxel treatment for 48 hrs (paclitaxel concentrations were 6 nM in HeyA8, 5nM in SKOV3ip and 6nM in OVCAR5, respectively), and then collected for cell cycle and apoptosis analysis **(B and D)** Combination of EDN2 and TBK1 was tested in SKOV3ip, HeyA8 and OVCAR5 cell lines. Cell treatments and cell cycle/apoptosis analysis were carried out as described above. The columns indicate the mean, and the bars indicate the S.D. For A and C, \* $p < 0.05$  and \*\* $p < 0.01$ . For B, \*\*  $p < 0.01$  compared with siControl+Pac; ++  $p < 0.01$  compared to individual siRNA; ##  $p < 0.01$  compared to individual siRNA+Pac. For D, \*\*  $p < 0.01$  compared to siControl. Data were obtained from three independent experiments.

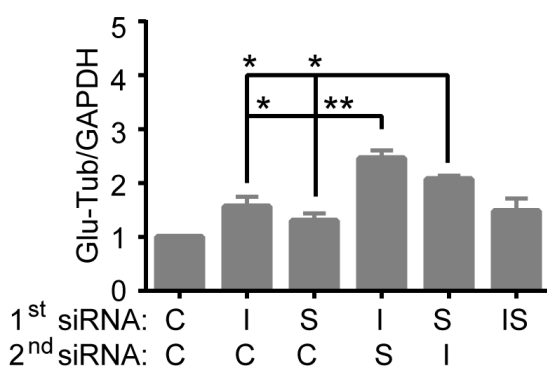
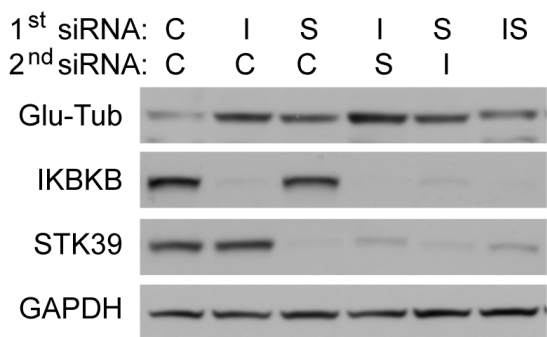
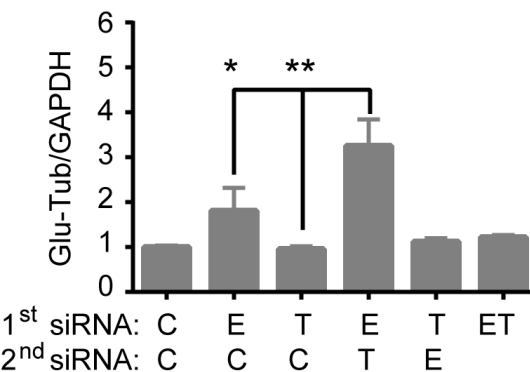
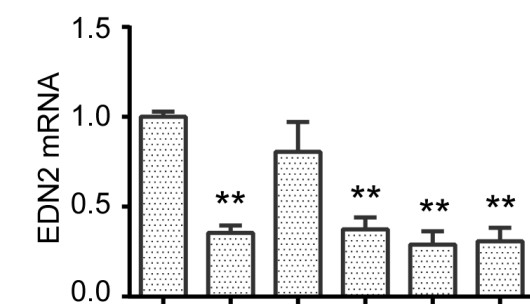
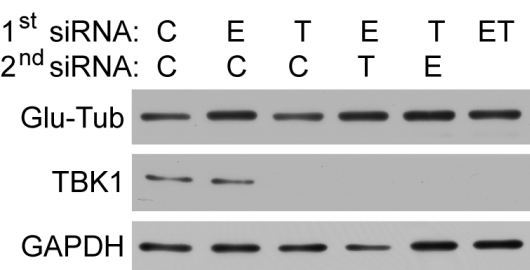
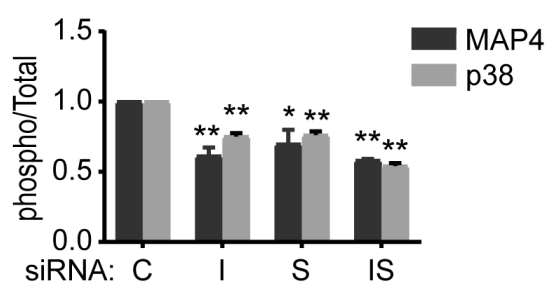
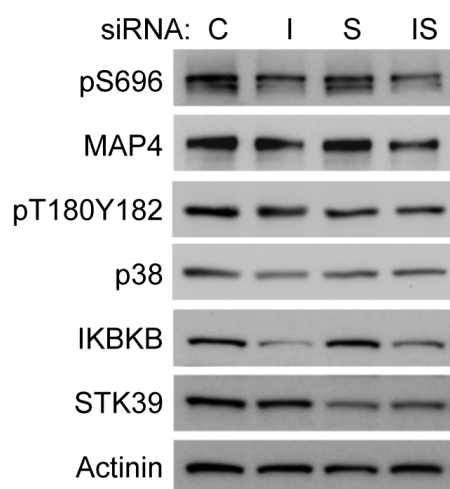
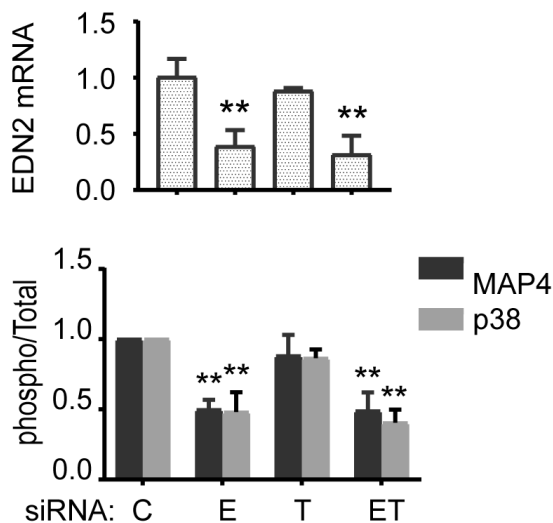
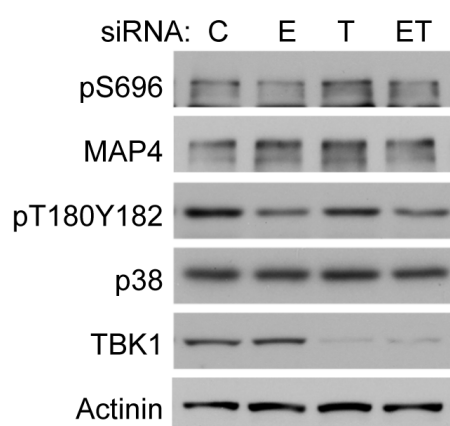
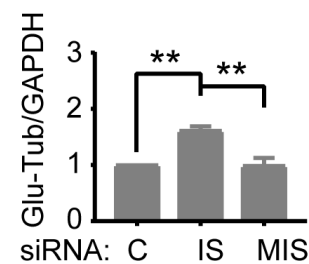
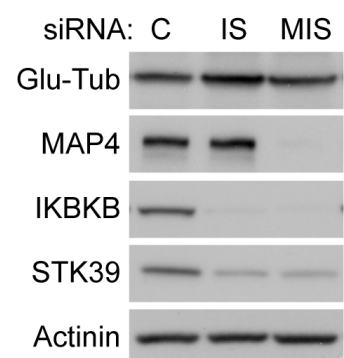
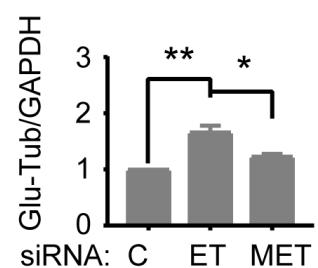
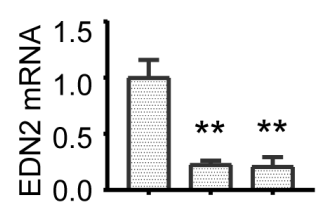
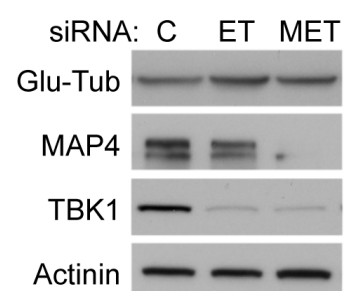
**Figure 5. Combination of IKBKB/STK39 and EDN2/TBK1 siRNAs sensitize paclitaxel in mice xenografts models.** **(A)** Combination treatment with IKBKB/STK39 was examined in SKOV3ip and OVCAR5 xenograft models. Athymic nude mice were injected intraperitoneally with  $1.0 \times 10^6$  SKOV3ip cells or  $1 \times 10^6$  OVCAR5 cells and randomly assigned to groups of 10. Mice were treated with paclitaxel and/or DOPC-siRNA beginning 1-week after cell inoculation. 10 ug of siRNA was injected i.p. biweekly and 1 mg/kg of paclitaxel for SKOV3ip or 3 mg/kg for OVCAR5 or diluent were injected i.p. once a week. Tumor weight was assessed immediately after mice were euthanized. **(B)** Combination treatment of EDN2 and TBK1 was examined in SKOV3ip xenograft models. Cell inoculation and mice treatment were conducted as described above. The columns indicate the mean, and the bars indicate the S.E. (\* $p < 0.05$  compared with control).

**Figure 6. IKBKB and STK39 are overexpressed in ovarian cancer and related to poor prognosis.** (A) Ovarian cancer tissue microarrays (TMA) were examined using Immunohistochemical analysis. Representative images of normal and ovarian cancer TMAs are presented. (B) The percentage of negative and positive case for either IKBKB or STK39 were calculated and plotted. (C) Survival curves based on expression were generated using Kaplan-Meier method and the prognostic comparison of low vs high expression was calculated using Logrank Mantel-Cox test (Graphpad).

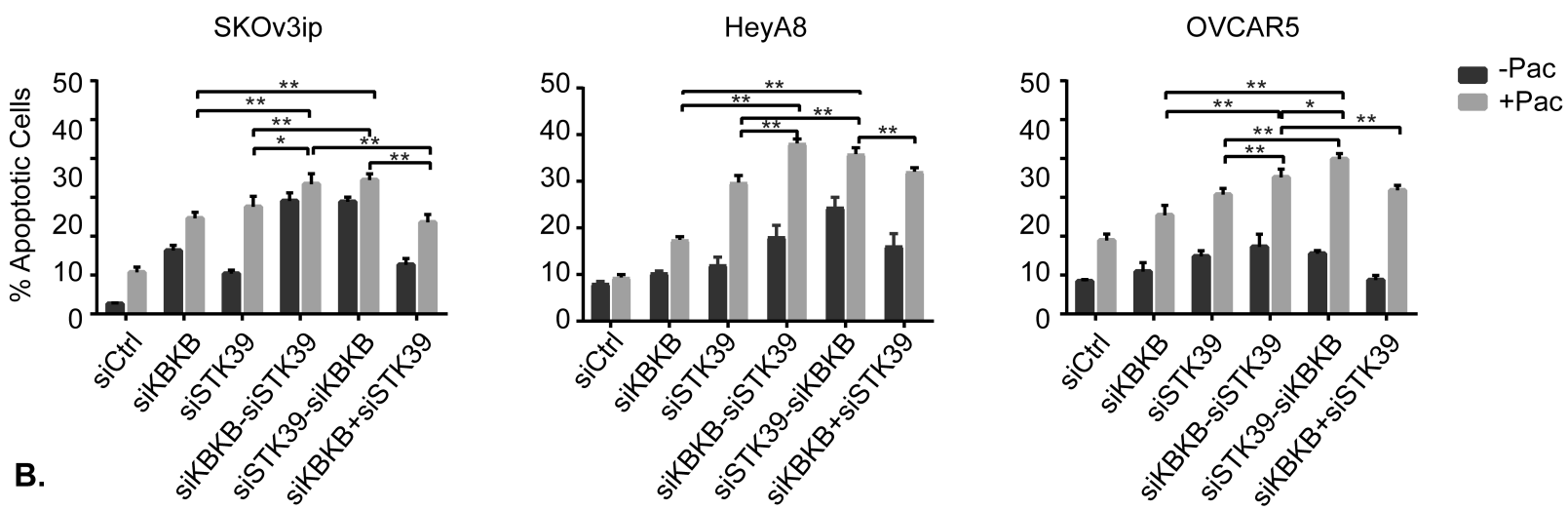
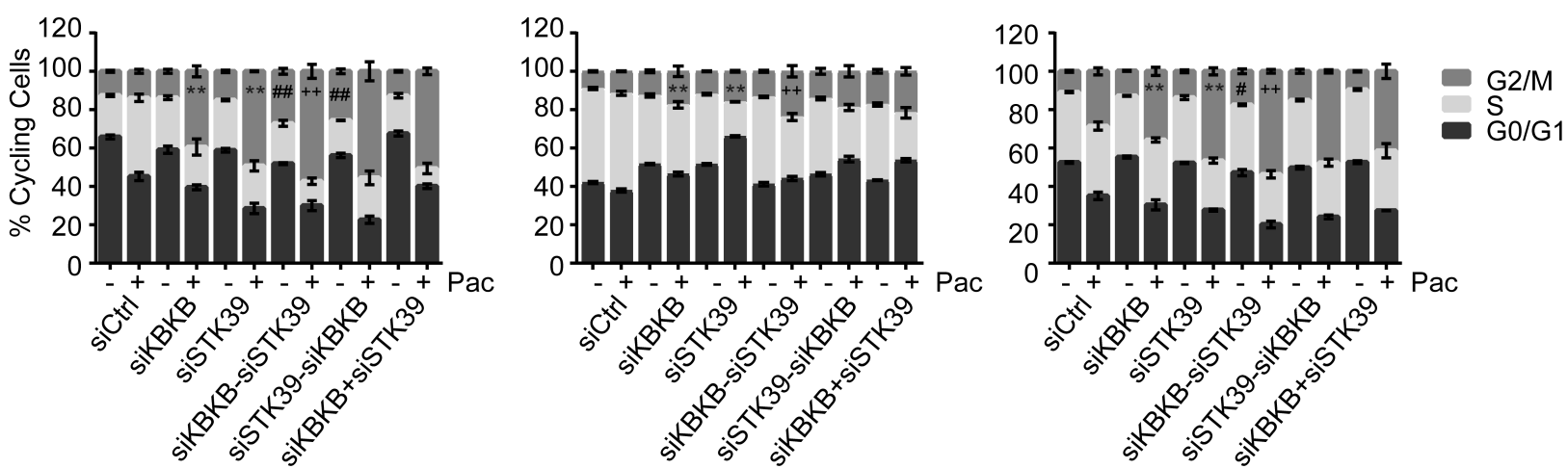
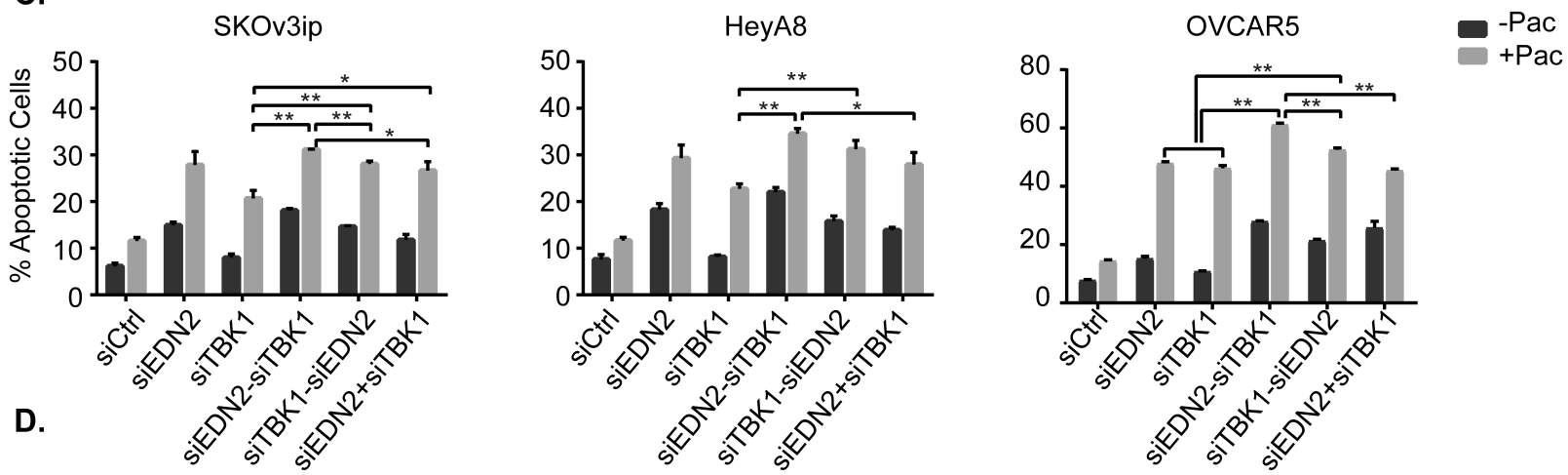
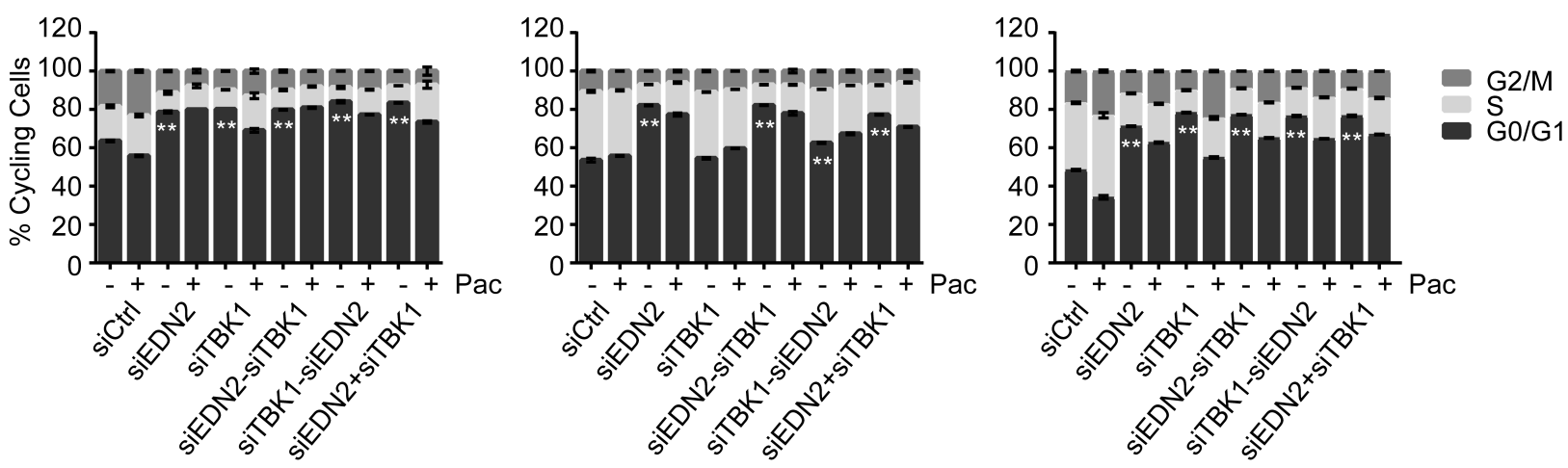
Figure 1

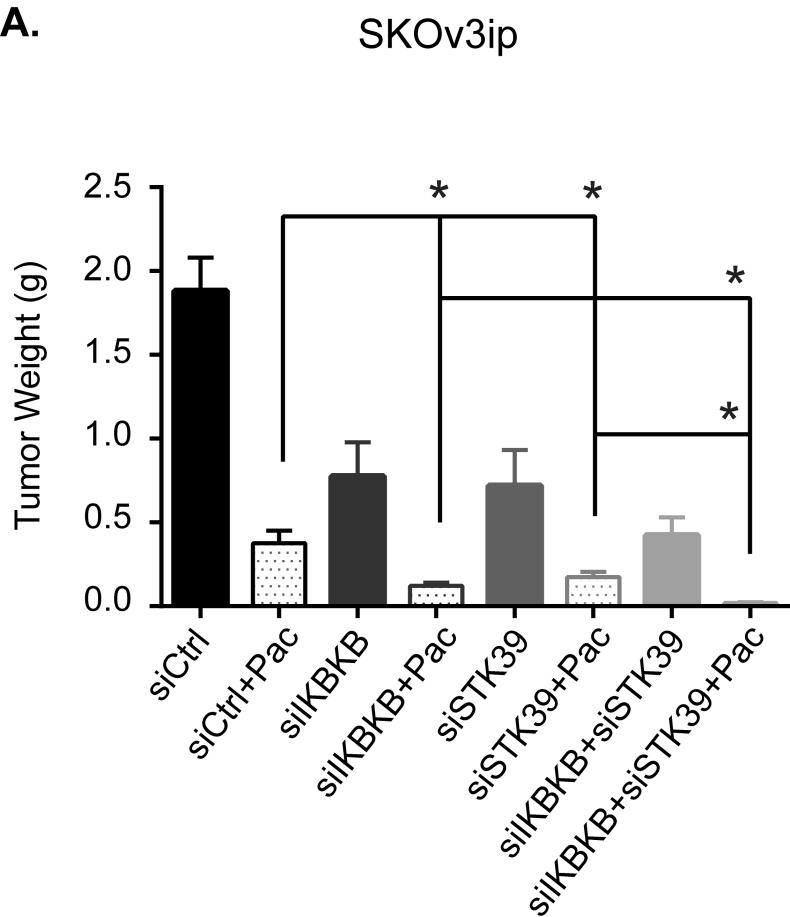




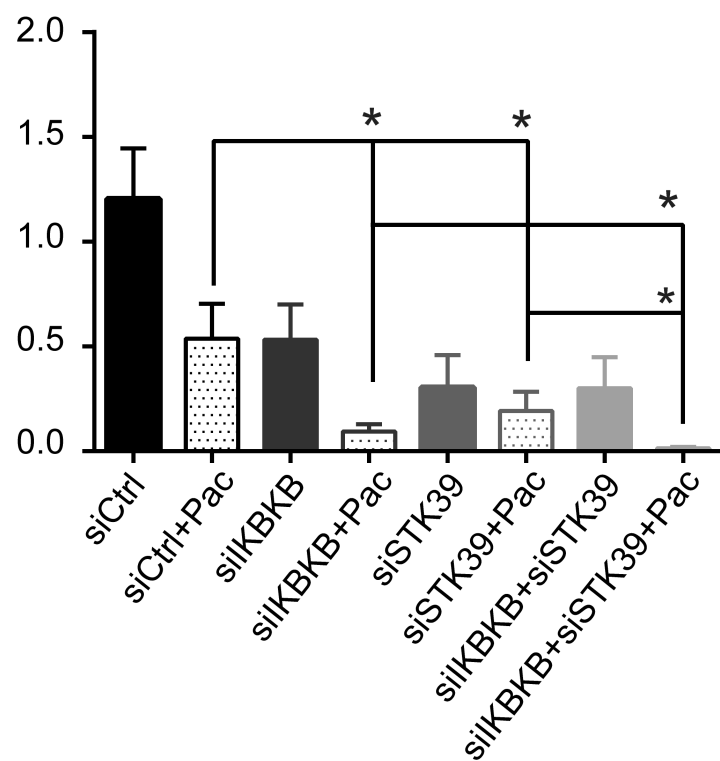
**A.****B.****C.****D.****E.****F.**



**A.****B.****C.****D.**

**A.**

OVCAR5

**B.**